Chemical Application of Silicon-Based Resonant Microsensor

A Thesis
Presented to
The Academic Faculty

by

Albert Byun

In Partial Fulfillment
of the Requirements for the Degree
Master of Science in the
School of Electrical and Computer Engineering

Georgia Institute of Technology
August 2007

Chemical Application of Silicon-Based Resonant Microsensor

Approved by:

Dr. Oliver Brand, Advisor
School of Electrical and Computer Engineering
Georgia Institute of Technology

Dr. Boris Mizaikoff
School of Chemistry and Biochemistry
Georgia Institute of Technology

Dr. Bruno Frazier
School of Electrical and Computer Engineering
Georgia Institute of Technology

Date Approved: May 16, 2007

Dedicated to my beloved family

ACKNOWLEDGEMENTS

I would like to express my gratitude to all those who helped me complete my thesis. I am deeply indebted to my advisor, Dr. Oliver Brand who has been motivating, encouraging and supportive in all these times. I greatly appreciate the sincere support of Dr. Boris Mizaikoff who provided enthusiastic and critical suggestions during our academic collaboration. I am very grateful to Dr. Bruno Frazier whose academic endeavor largely expanded my horizons. Very special thanks to Jeo Hyeong Seo for the intellectually stimulating and valuable advices, without whose help I could have never come this far.

I want to specially thank those who help me go through the hard times: Gary Dobbs and Yulia Luzinova who did not hesitate a single moment providing me with constructive advices and mentoring on many occasions.

Especially, I thank my loving parents who I most admire and aspire to live and love like, and my beloved sister who stood by my side through all these years. Last but not least, I sincerely appreciate Jayoung Sung's support throughout my years at Georgia Tech.

TABLE OF CONTENTS

ACKNOWLEDGEMENTS ..... **IV**

LIST OF TABLES ..... **VII**

LIST OF FIGURES ..... **VIII**

SUMMARY ..... **X**

CHAPTER 1: INTRODUCTION **1**

1.1 MOTIVATION AND BACKGROUND 1

1.2 MASS SENSITIVE CHEMICAL MICROSENSORS 2

CHAPTER 2: MASS-SENSITIVE MICROSENSORS IN LIQUID **4**

2.1 SENSING IN LIQUID ENVIRONMENT 4

2.2 DISK-SHAPE RESONATOR FOR LIQUID MEASUREMENT 7

CHAPTER 3: POLYMERS AS SENSITIVE LAYERS **10**

3.1 SOURCES OF ADHESION 10

3.2 ADHESION ISSUES IN LIQUID ENVIRONMENT 11

3.3 POLYMER COATING PROTOCOLS 14

3.4 ADHESION TESTS USING ULTRASONIC BATH 18

CHAPTER 4: LIQUID PHASE MEASUREMENTS **24**

4.1 MEASUREMENT AND COATING SETUP 24

4.1.1 Flow Cell Design 25
4.1.2 Customized Coating System 28
4.2 MEASUREMENT RESULTS 29
4.2.1 Analytical Calculation of Resonance Frequency after Polymer Coating 30
4.2.2 Estimation of Detection Limit 31
4.2.3 Measurements with PVP Polymer Coating 33
4.2.4 Measurements with EPCO Polymer Coating 38
4.2.5 Testing of Uncoated Resonator in Liquid Flow Cell 43
CHAPTER 5: CONCLUSIONS AND RECOMENDATIONS 46
5.1 CONCLUSIONS 46
5.2 RECOMMENDATIONS FOR FUTURE WORK 50
REFERENCES 51

LIST OF TABLES

Table 4. 1: Calculation of detection limit using the Allan Variance data (* the enrichment factor for PVP is estimated and needs to be verified experimentally)..... 32

LIST OF FIGURES

Figure 2.1: (a) Strain and (b) stress distribution as obtained by finite element simulation for in-plane mode shape of disk-type resonator investigated in this work. 8

Figure 3. 1: Resonator coated with EPCO sensitive film (a) before operation in de-ionized water and (b) after operation in de-ionized water for one hour. 12

Figure 3. 2: Surface reaction between OH groups on the surface of a silicon dioxide film and a silane coupling agent. The subscript "S" denotes the substrate. 16

Figure 3.3: Photographs of wafer samples with Si_3N_4 or SiO_2 passivation coated with PVP (physical coating protocol) (a) before and (b) after exposure ultrasonic bath..... 19

Figure 3.4: Photographs of wafer samples with Si_3N_4 or SiO_2 passivation in case of grafting-to chemical coating protocol using (a) PVP and (b) EPCO after exposure to the ultrasonic bath. 20

Figure 3.5: Photographs of wafer samples with Si_3N_4 or SiO_2 passivation in case of grafting-from chemical coating protocol with SBR (a) before and (b) after ultrasonic bath. 20

Figure 3.6: SBR coating on a SiO_2 surface after exposure to the ultrasonic bath: (a) SEM image, (b) profilometer measurement showing a remaining film thickness of approx. 70nm. 22

Figure 4.1: 3D view of designed flow cell (a) before and (b) after assembly. 26

Figure 4. 2: Three components of designed flow cell..... 26

Figure 4. 3: (a) Fabricated flow cell components and the DIL package with bonded resonator chip and (b) overall setup with flow cell mounted to circuit board holding the feedback circuitry..... 27

Figure 4. 4: Customized coating setup attached to wire bonder. 28

Figure 4. 5: Polymer film thickness calculated from the resonance frequency change before and after coating as a function of the polymer concentration in the solvent. 31

Figure 4. 6: Magnitude and phase transfer characteristic in air around in-plane resonance mode (a) before and (b) after coating with PVP film. 34

Figure 4. 7: Photographs of disk-type resonator taken (a) before coating, (b) after coating with 0.5% PVP, and (c) after liquid measurement..... 35

Figure 4. 8: Resonance frequency of disk-shape resonator coated with PVP film in water subject to periodic injection of 30ppm TeCE. 36

Figure 4. 9: Magnitude and phase transfer characteristic in air around in-plane resonance mode (a) before and (b) after coating with PVP film deposited from 1% PVP solution.. 37

Figure 4. 10: Photographs of disk-type resonator taken (a) before coating, (b) after coating with 1% PVP and liquid measurement..... 37

Figure 4. 11: Resonance frequency of disk-shape resonator coated with PVP film (deposited from 1% PVP solution) in water subject to periodic injection of 150ppm TeCE. 38

Figure 4. 12: Magnitude and phase transfer characteristic in air around in-plane resonance mode (a) before and (b) after coating with EPCO film deposited from 0.5% EPCO solution in hexane. 39

Figure 4. 13: Photographs of disk-type resonator taken (a) before coating, (b) after coating with 0.5% EPCO solution and (c) after liquid measurement. 40

Figure 4. 14: Resonance frequency of disk-shape resonator coated with EPCO film (deposited from 0.5% EPCO solution) in water subject to periodic injection of 150ppm TeCE. 41

Figure 4. 15: Magnitude and phase transfer characteristic in air around in-plane resonance mode (a) before and (b) after coating with EPCO film deposited from 0.1% EPCO solution in hexane. 42

Figure 4. 16: Photographs of disk-type resonator taken (a) before coating, (b) after coating with 0.1% EPCO solution and (c) after liquid measurement. 42

Figure 4. 17: Measured resonance frequency during 100s period for EPCO-coated resonator (deposited from 0.1% EPCO solution). 43

Figure 4. 18: Frequency measurement of uncoated resonator during equilibration in liquid flow cell with 10µl/min flow rate. 44

Figure 4. 19: Measured resonance frequency during 100s period for uncoated resonator. 45

SUMMARY

The detection of volatile organic compounds in liquid is of interest for applications in public health, workplace safety and environmental monitoring. Traditionally, water samples were taken and analyzed in the laboratory using classical laboratory instrumentation. Current trends target real-time measurements using e.g. chemical microsensors built with microfabrication technologies. Among these, mass-sensitive chemical sensors, based on cantilever beams or surface acoustic devices, have shown substantial promise in gas-phase applications. In a liquid environment, the resonant microstructures typically suffer from high damping, which negatively affects the sensor resolution. In this work, a novel disk-type resonator developed at Georgia Tech was investigated as chemical microsensor for liquid-phase applications. The micromachined resonator vibrates in a rotational in-plane mode shape, reducing damping in a liquid environment. As part of the present research, a measurement setup with a custom-made flow cell for liquid-phase chemical measurements and a coating system to locally deposit polymer sensitive films onto the resonators were developed. To improve the film adhesion on the resonator surface in liquid, physical and chemical binding techniques were developed and tested on wafer samples. Polymers such as poly(4-vinylpyrrolidone), poly(ethylene-co-propylene) and poly(styrene-co-butadiene) were deposited using the custom-designed coating system onto the disk-type resonators. Liquid-phase measurements using tetrachloroethylene as the chemical analyte were performed. The experimental results are discussed, sources of problems are identified and recommendations for future research are made.

CHAPTER 1

INTRODUCTION

1.1 Motivation and Background

The exponential growth in integrated circuit fabrication technologies offers opportunities for the development of small size microsensors using similar microfabrication processes. Advantages of using these fabrication techniques include the reduction of the transducer size, batch processing and the option of integrating signal processing circuitry. The use of batch fabrication techniques substantially reduces the production cost per device in case of high-volume products without sacrificing manufacturing tolerances [1]. These substantial benefits have created a new wave in developing sensors using microfabrication technique.

Chemical microsensors are investigated for applications in public health and environmental monitoring [2], offering fast response times, high sensitivity and selectivity. Monitoring clinically important measurands in real-time and detecting toxic chemicals in the air or drinking water are two areas where chemical microsensors are considered as viable solutions.

In modern analytical chemistry, many tasks are difficult to solve with classical laboratory instruments, requiring small size, fast and low-cost instruments without sacrificing sensitivity and selectivity. Because of their small size, chemical microsensor probes smaller sample volumes and can be used as localized probes.

To enhance the sensor selectivity, multiple chemical microsensors can be integrated onto a single smart chip that simultaneously probes air samples using three complementary transduction mechanisms [3]. The microsensor system responds to the mass of absorbed molecules, the heat of absorption, and the volume and dielectric properties of the absorbents. In order to release the micromechanical components of these integrated sensing systems, microelectromechanical systems (MEMS) fabrication processes such as surface or bulk micromachining compatible are inserted either prior to, in the middle of, or after CMOS fabrication processes [4]. Such merged fabrication processes drive integrated MEMS devices to industrial mass production.

To date, most chemical microsensor technologies have been demonstrated in an ideal laboratory environment. Additional efforts are needed to ensure the robustness of the sensing principles (e.g. sensitivity, selectivity, and resolution) in the field with typically increased noise levels and impact of variable ambient conditions. At the same time, the dynamic range of the input signal and the system stability over time must not be sacrificed under extreme environmental conditions [5]. Needless to say, real-time and continuous measurements are the additional requirements for portable applications. Up to now, issues related to high initial cost for a fabrication environment, insufficient long-term stability, sensitivity and selectivity have been barriers to the wide commercialization of MEMS-based chemical microsensors.

1.2 Mass Sensitive Chemical Microsensors

Chemical sensors convert changes in the physicochemical properties of a sensitive layer into electrical signals that can be used for further data processing. The sensitive

layer interacts with chemical species through absorption, chemical reaction, enrichment and/or charge transfer [1]. Depending on the transduction principles, chemical sensors are categorized into thermal, mass-sensitive, electrochemical (i.e. potentiometric, amperometric, or conductometric), and optical sensors [6].

Mass changes can be detected by either observing the deflection of a micromechanical structure due to mass-loading or surface-stress changes (static mode), or by monitoring frequency changes of a resonating structure or a propagating acoustic wave upon mass loading (dynamic mode) [1]. Cantilevers are widely used as micromechanical sensing elements. In the static mode operation, the cantilever deflection is measured by sensing a laser beam reflected off the cantilever tip with a position-sensitive detector [7]. In dynamic mode operation, changes in the resonance frequency of the micromechanical structure are correlated to the added mass of the structure [8]. In case of the cantilever beam, transverse beam vibrations at a resonance mode are generated by either electro-thermal excitation with integrated heating resistors or magnetic excitation based on the Lorentz force [4]. Analytes absorbed into a sensing layer deposited on top of the cantilever increase its mass and thus decrease its resonance frequency. The beam vibrations in the dynamic mode are sensed by e.g. four piezoresistors arranged in a Wheatstone bridge configuration located in the region of maximum stress of the resonating structure.

In the present work, a new type of integrated mass-sensitive transducers vibrating in a rotational in-plane mode shape is investigated as a chemical microsensor for liquid operation.

CHAPTER 2

MASS-SENSITIVE MICROSENSORS IN LIQUID

2.1 Sensing in Liquid Environment

To monitor water pollution and ensure the safety of our drinking water, chemical microsensors that can operate in liquid are desirable. Among others, suitable microsensors must provide detection limits in the parts-per-million range (or even below) to be applicable for pollutant sensing in water. Currently, the most common mass sensors operating in liquid are Quartz Crystal Microbalances (QCM), surface acoustic wave (SAW) devices [9] and cantilever-based sensors.

The QCM devices, also known as bulk wave or thickness shear mode (TSM) devices, utilize a bulk shear wave formed between the two surfaces of a piezoelectric disk. Typically, AT-cut quartz is used as piezoelectric substrate. The operating frequency is determined by the thickness of the piezoelectric disk. The piezoelectric coupling and elastic stiffness constants determine the displacement of the acoustic wave [10]. The quality factor of the resonance frequency, which ultimately limits the sensor resolution for resonant sensors with a frequency output, can exceed 100,000 in air.

SAW devices are based on acoustic waves traveling on the surface of a substrate from a sensing element to a receiving element. Again, the piezoelectric effect is widely used to excite and sense the acoustic wave. Either, a piezoelectric substrate and a piezoelectric thin film deposited onto the substrate can be used. The operating frequency of SAW devices is generally higher than that of QCM devices and hence, SAW devices

typically have better sensitivity. On the other hand, the frequency response of SAW devices is an accumulation of mass loading as well as modulus changes of the active layer. This phenomenon is mainly due to the polymer swelling which may be the dominant factor in the transduction mechanism as supported in a number of experiments [9]. If the SAW device substrate has a sufficient electromechanical coupling constant, and if the sheet conductivity is within a certain range, acoustoelectric interaction occurs that can lead to changes in the acoustic wave velocity and alterations in the oscillation frequency of the circuit [10].

For acoustic wave devices, the velocity of the acoustic wave and the direction of particle displacement at the surface determine the feasibility of liquid operation. If surface normal displacements occur, and if the acoustic wave velocity is greater than the compressed sound wave in the liquid, the propagating acoustic wave undergoes a severe attenuation. Thus, acoustic wave devices operating in shear horizontal motion, i.e. surface displacements in wave propagation direction and parallel to the sensing surface, are preferable for liquid measurements. Besides the thickness shear mode (TSM) resonators discussed earlier, surface transverse wave (STW), leaky SAW, Love wave and shear-horizontal acoustic plate mode devices qualify for operation in liquid [9]. TSM devices have been adopted for commercial applications and TSM-based biosensors were developed for the detection of sugar molecules and DNA hybridization [9].

Acoustic wave devices using viscoelastic polymer sensing layers suffer from a modulus effect that leads to sensor signals due to polymer thermal expansion, chain relaxation processes and film resonance. An increasing temperature enlarges the polymer volume due to the non-zero thermal expansion coefficient of polymers, decreases chain to

chain interactions, which lowers the polymer modulus and, thus, reduces the acoustic wave velocities, which ultimately leads to a decrease in the observed frequency. Once the acoustic wave displaces the polymer, the relaxation time of polymer chains depend on the temperature and the structure of the particular polymer. Based on the polymer relaxation time and the period of the probing ultrasonic wave, the effective modulus of the polymer layer undergoes a dynamic glass-to-rubber transition. As a consequence, the effective modulus drops and the amplitude attenuates as energy gets coupled into the polymer film and dissipated under these conditions [9].

The material properties of the polymer sensing layer also affect the analyte diffusion into the coating that governs the dynamic behavior of the sensor response. Studies have shown that glassy polymers, which operate below their glass transition temperature, respond much slower to analyte concentration changes and exhibit smaller frequency shift, indicating smaller analyte enrichment factors. On the other hand, rubbery polymer coatings with a glass transition temperature below the operating temperature exhibit greater free volume as well as polymer chain segmental motion that results in faster analyte diffusion and higher sensitivity. The response of sensors with rubbery polymer coatings is a combination of both the mass loading of absorbed analyte and the accompanying decrease in the coating's shear parameter. This viscoelastic effect is hard to avoid if the coating thickness exceeds a material dependent value [11, 12]. In case of the QCM device, it was observed that under certain conditions, the viscoelastic effect increased the resonant frequency and exceeded the mass effect, resulting in a positive frequency shift upon analyte absorption [12].

2.2 Disk-Shape Resonator for Liquid Measurement

The sensing principle of a mass-sensitive resonant microsensor is based on the fact that the effective mass of the resonant structure is changed by the absorption/desoprtion of target analytes, resulting in a change of the structures resonance frequency. Resonant microsensors can generally be modeled by a simple harmonic oscillator consisting of the structural effective mass m, effective spring constant k, and damping coefficient b. Assuming a driving force F, the equation of motion is given by:

$$kx + m\frac{d^2x}{dt^2} + b\frac{dx}{dt} = F \tag{2.1}$$

Then, the resonance frequency, i.e. the frequency of maximum amplitude of the transfer function $\frac{\bar{x}}{\bar{F}}$, is given by

$$f_0 = \frac{1}{2\pi}\sqrt{\frac{k}{m}} \tag{2.2}$$

Assuming the stiffness change of the structure due to analyte absorption is negligible, the relative resonance frequency shift of a microstructure upon mass loading can be further expressed as

$$\frac{\Delta f}{f_0} = -\frac{1}{2}\frac{\Delta m}{m} \tag{2.3}$$

where Δf and Δm represent frequency shift and mass variation of a resonator, respectively. Hence, the change in resonance frequency is proportional to the added mass in the sensing layer [13]. Similar equations can be derived in case of a rotational instead

of a translational oscillation. In this case, the spring constant is given by the rotational spring constant and the mass be the rotational moment of inertia.

In liquid environment, cantilever-type resonators undergo significant damping due to their out-of-plane vibration modes. As a result, the quality factor is substantially degraded, thus deteriorating the mass sensitivity of the device. In order to minimize the effect of damping in liquid, a disk-shape resonator oscillating in a rotating in-plane-mode shape has been developed recently at Georgia Tech [14]. The measured quality factor of the device in water is approximately 100, which is considerably higher than values typically found for cantilever-based sensors [15]. Figure 2.1 illustrates the shape of the disk-type resonator and its in-plane vibration mode with both semi-disks vibrating in phase. The disk-type resonator features two semi-disks that are connected to a central anchor beam by two support bars.

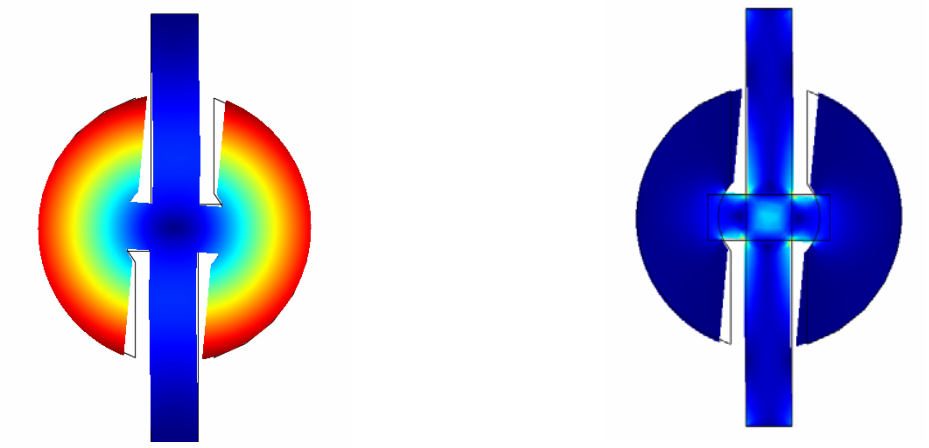

(a) (b)

Figure 2.1: (a) Strain and (b) stress distribution as obtained by finite element simulation for in-plane mode shape of disk-type resonator investigated in this work.

Integrated heating resistors placed asymmetrically at the edge of the support bars generate the required rotational torque to excite the in-plane rotation. Only the in-plane vibration is detected by arranging four piezoresistors in a Wheatstone bridge configuration in the center of the anchor beam where maximum stress occurs. The physical dimensions of the disc-shape resonator determine the resonant frequency and quality factor of the device [13].

The resonator is incorporated as the frequency-determining element in a self-oscillating amplifying feedback loop consisting of a series of amplifiers, a phase shifter, and a Schmitt Trigger used as a comparator. The output from the comparator excites the resonator and compensates the damping term in Eq. 2.1, enabling continuous operation with constant vibration amplitude at the resonance

CHAPTER 3

POLYMERS AS SENSITIVE LAYERS

3.1 Sources of Adhesion

Operation in a liquid environment imposes additional restrictions on the material properties of the polymer film functioning as the sensitive layer. The ideal polymer film should be insoluble and immune to swelling and delaminating in (water-based) liquids, easily and reproducibly deposited on the resonator, and resistant to irreversible chemical or physical changes from the target analytes. In order to implement a successful measurement protocol, the sensor response should be linearly related to the analyte concentration, and have fast response times for continuous measurement. At the same time, the sensitive layer should be insensitive to variations in the physical measurement conditions, such as temperature, flow rate, mechanical and electrical liquid properties [11].

In order to understand the delaminating behavior in water, it is important to understand the source of adhesion at the interface between sensitive layer and resonator surface. The intrinsic adhesion originates from interlocking of the adhesive into the irregular surface of the substrate, which is also known as mechanical keying. It was observed that joint strength improved when a microfibrous surface topology was created. For instance, in studies on the adhesion of polyethylene to metallic substrates [15], high peel strengths were obtained when a very rough and microfibrous oxide surface was created on the surface. An alternative explanation to the mechanical keying is the

diffusion theory associating inter-diffusion of polymer and substrate molecules across the interface [15]. When certain metals are evaporated or sputtered on polymeric substances, inter-diffusion seems to act as the main source of adhesion. More specifically, atomic interfacial mixing builds an interface region between the polymer and the metallic substrate, if ion implantation and plasma polymerization techniques are used [15].

Surface energy is an important determinant in the adhesion of polymers to silicon substrates. The surface energy is a measure of the disruption of chemical bonds that occurs when a surface is created. Organic compounds, such as polymers, are characterized by low-energy surfaces, while metals, metal oxides, and ceramics have high-energy surfaces. Since water has a strong capacity for bonding, hydrophilic surfaces have higher surface energies compared to hydrophobic surfaces [15]. In a liquid environment, the water concentration near the interface decreases as the surface hydrophobicity increases, resulting in a better film adhesion [16].

3.2 Adhesion Issues in Liquid Environment

The initial polymer coating and chemical analyte pair selected in this work for liquid-phase chemical measurements were polyethylene-co-propylene (EPCO) and tetrachloroethylene (TeCE), respectively. The EPCO film was dispensed onto the resonator using a custom designed coating system (see Chapter 4.1.2). After operating the coated resonator in de-ionized (DI) water for an hour, it was found that the polymer coating delaminated from the resonator surface, as shown in Figure 3.1.

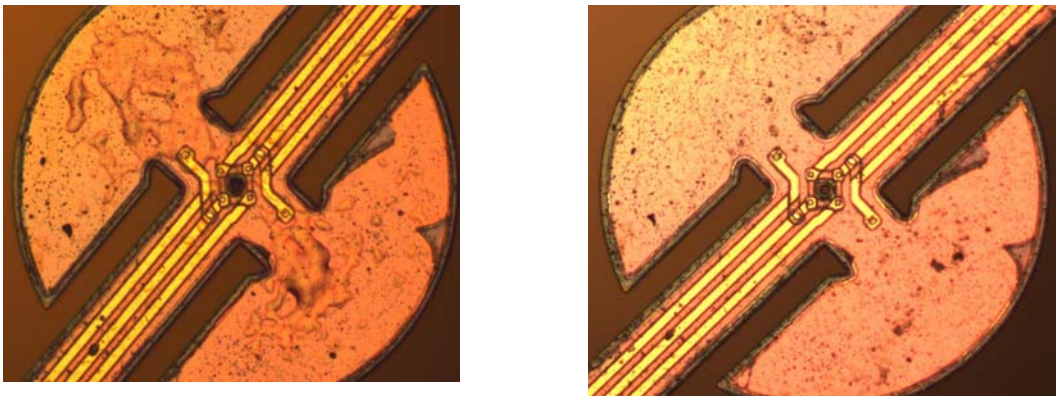

(a) (b)

Figure 3. 1: Resonator coated with EPCO sensitive film (a) before operation in de-ionized water and (b) after operation in de-ionized water for one hour.

Studies have shown that moisture accumulation at the interface between polymer and silicon surface leads to considerable loss in strength of adhesive joints [16-19]. We speculate that the observed adhesion loss results from the two following reasons: water diffusion into the bulk polymer and water penetration along the interface [17]. The water diffusion causes a film aging and a reduction in the mechanical properties of polymer, such as the Young's modulus. The interfacial water generally seeps at a faster rate than the water diffusion across the bulk polymer. Therefore, not only the material properties of the polymer itself are important, but also minimizing the exposure of the interface layer to ambient water is critical for maintaining good adhesion properties over time.

Proper surface treatment is a crucial factor for controlling interfacial diffusion. Water penetration along the interface is associated with progressive bond breaking at the interface and with water diffusion in the adhesive used to join the surfaces. Alternatively, structural changes across the interface from the polymer to the substrate might cause an enhanced diffusion along the interfacial region [17].

Interestingly, the moisture content at the polymer/substrate interface appears to be strongly dependent upon the underlying substrate surface chemistry and independent on the polymer [16]. This also indicates that interfacial chemistry plays a dominant role in adhesion failure. The water concentration near the surface decreases as the surface becomes more hydrophobic. However, when comparing between dry and wet adhesion of hydrophobic and hydrophilic surfaces, an increase in hydrophobicity inevitably leads to inferior adhesion strength in air (dry adhesion), while the adhesion improves in water (wet adhesion), as discussed earlier [16].

Silane-based coupling agents are often used in microelectronics to improve adhesion between inorganic oxides and polymers [18]. Depending on the thickness of the binding material at the interface, the silane adhesion promoter, also called the coupling agent, functions as a surface modifier, primer and an adhesive. A coupling agent with a thickness close to a monolayer chemically modifies the substrate surface without contributing any mechanical film properties of its own. As the thickness increases, adequate mechanical film properties such as rigidity, tensile strength and toughness contribute to the mechanical loading [20]. In a previous study [19], wet adhesion tests were performed on epoxy coatings deposited on silane-treated and untreated silicon surfaces in order to estimate the moisture build-up at the interface. Fourier Transform Infrared-Multiple Internal Reflection (FTIR-MIR) spectroscopy was used to measure the water layer thickness at the interface. Little water was observed at the interface of the silane-treated samples, while approximately 10 monolayers of water had accumulated at the interface of the untreated samples after 100 hours of exposure to 24˚C water. Within 75 hours of exposure, the epoxy films on the untreated substrates lost most of their

bonding strengths, whereas the silane-treated specimens retained 80% of their adhesion after 600 hour of exposure. The adhesion loss was highly correlated to the interfacial water build-up. Coherently, the bond strengths between the substrate surface and the epoxy resin were stronger for the treated surface [19]. The source of the adhesion loss on silane-treated surfaces was mainly attributed to the hydrolysis of the silane layer [18].

Hence, the moisture buildup at the interface has been identified as the primary cause of delamination of the polymer coating in the initial measurement. Depending on the material properties of polymer coating, appropriate surface treatment techniques are introduced to minimize water penetration through the interface and lead to stronger adhesion strength in water.

3.3 Polymer Coating Protocols

The analyte enrichment into a polymeric film depends (among others) on the glass transition temperature of the polymer relative to the operating temperature. Polymers are considered glassy if the glass transition temperature is higher than the operating temperature. On the other hand, rubbery polymers have a glass transition temperature below the operating temperature. Experiments on the detection of organic pollutants in water with thickness-shear-mode (TSM) resonators have shown[11, 12] that rubbery polymers resulted in higher sensitivities and generally a more reversible and faster sensor response. The associated faster analyte diffusion is the result of a larger free volume and polymer chain segmental motion above the glass transition temperature. In addition to the mass increase from the analyte diffusion, rubbery polymers exhibit an accompanying decrease in the coating's shear parameters. If the coating thickness exceeds a material-

dependent value, viscoelastic effects were observed to affect the sensor measurement [11, 12]. In contrast, glassy polymers behaved more like a rigid material, but exhibiting low sensitivities leading to small frequency shifts and slow sensor responses.

In the present work, the following polymers have been investigated as sensitive layers: poly(4-vinylpyrrolidone) (PVP), poly(ethylene-co-propylene) (EPCO), and poly(styrene-co-butadiene) (SBR).

PVP is well known for its good adhesion characteristics in water and has been chosen in this work for the purpose of enhancing the physical film adhesion. Some of the undesirable characteristics are that the polymer is water-soluble and that it has a glass transition temperature close to 184˚C [21], making it as glassy polymer. PVP can become insoluble in water after cross-linking to the substrate.

EPCO and SBR have been selected due to their inert properties in water. Dr. Mizaikoff's research group at Georgia Tech have extensive experience with both polymers and has characterized them in water using infrared spectroscopy. At the operating temperature of 24˚C, both polymers show rubbery characteristics as their glass transition temperatures are below or close to the operating temperature. The glass transition temperature of EPCO is in the range between 0˚C and 20˚C [22], the one of SBR is in the range between 25˚C and 30˚C [23].

Two types of adhesion methods, namely physical adhesion and chemical bonding, were investigated in this work. In case of chemical binding, two basic techniques, grafting-to and grafting-from, are used to bind the films to the substrate. In the grafting-to method, the binding occurs between polymer chains with specific functional groups along the chain or at the chain ends and appropriate functional groups on the substrate. Long

reaction times (over 24 hours) are often needed with this method. In the grafting-from method, polymers are grown on the substrate, yielding good control of layer thickness and surface composition [24]. All three methods have been investigated for the polymer coating on top of the disk-shape resonator.

Silane coupling agents create chemical bonds between the polymer and the substrate and have been used in the grafting-to approach. Hexamethyldisilazane (HMDS) is commonly used as an adhesion promoter in photolithographic processes and reacts with the OH groups on the surface of silicon dioxide films [25]. Based on this study, HMDS is considerably more reactive than any other silane previously studied. The overall chemical reaction taking place at the silicon dioxide surface is summarized in Figure 3.2.

$$2Si_S - OH + (CH_3)_3Si - \underset{\displaystyle H}{\underset{|}{N}} - Si(CH_3)_3 = 2Si_S - O - Si(CH_3)_3 + NH_3$$

Figure 3. 2: Surface reaction between OH groups on the surface of a silicon dioxide film and a silane coupling agent. The subscript "S" denotes the substrate.

Alternative to using a silane coupling agent, a chemical bonding protocol is used to bond SBR to the resonator surface. The protocol induces covalent bonds between the polymer and a promoter, which itself is covalently bonded to the silanized silicon surface. In the chemical bonding method, benzophenone was used as a photo-initiator cross-

linking octadecyltrichlorosilane and SBR. The presence of benzophenone greatly enhances the rate of cross-link formation. The highly cross-linked polymers are insoluble in water, and show improved physical properties [26].

All three coating methods have been tested using silicon oxide and silicon nitride wafer samples. The coating protocols are summarized in the following:

Physical Adhesion Method using PVP:

1. Clean wafer sample with toluene, acetone, ethanol, water, and ethanol in order.
2. Wait until the surface is completely dried.
3. Clean the wafer with oxygen plasma for 5 minutes.
4. Dissolve PVP in ethanol to form solution with defined weight concentration.
5. Coat PVP solution on wafer surface and wait until it is dried.
6. Cure polymer on surface for 4 hours in oven at 110°C.

Grafting-to Chemical Bonding Method using HMDS Coupling Agent:

1. Clean wafer sample with toluene, acetone, ethanol, water, and ethanol in order.
2. Wait until the surface is completely dried.
3. Spin coat hexamethyldisilizane (HMDS) at 3000 rpm for 40 seconds.
4. Cure on hot plate at 100˚C for 60 seconds.
5. Cool down sample to room temperature.
6. Drip coat polymer solution on the resonator surface.
7. Dry polymer at room temperature.

Grafting-from Chemical bonding Method using Benzophenone as a photoinitiator

1. Clean wafer sample with toluene, acetone, ethanol, water, and ethanol in order.
2. Wait until surface is completely dried.
3. Dissolve OTS in dry toluene to form a solution with a weight concentration of 3-4%.
4. Drip coat OTS solution on the surface and wait for 3 hours.
5. Dissolve styrene butadiene rubber (SBR), a copolymer, in toluene to form a solution with a weight concentration of 2%.
6. Mix benzophenone, a photo-initiator, with SBR solution (1% of SBR weight).
7. Drip coat the solution of SBR and benzophenone on the surface.
8. Wait for 1-3 hours until the film is dry.
9. Irradiate the sensor surface with UV light at 345μm wavelength.

3.4 Adhesion Tests using Ultrasonic Bath

The three polymer coating protocols described above were tested on 1cm by 1cm wafer samples with two possible surface passivation films: silicon dioxide and silicon nitride. Both films were deposited onto the silicon wafers using a Plasma Enhanced Chemical Vapor Deposition (PECVD) system and simulate the passivation layers normally used for the disk-type resonators. All samples were separately bottled in water-filled glass containers and mechanically stressed for 4 hours in an ultrasonic bath (Aquasonic Model 150D). Photographs of the coated wafer samples before and after treatment in the ultrasonic bath are given in Figures 3.3, 3.4, and 3.5. It should be noted that the mechanical stress introduced by the ultrasound bath is considered to far exceed

the mechanical stress normally encountered while operating the resonators in the rotational in-phase mode shape with typical vibration amplitudes in the nm-range. However, the coated wafer areas (1cm by 1cm) are large compared to the actual sensitive layer areas (typically 100µm by 100µm).

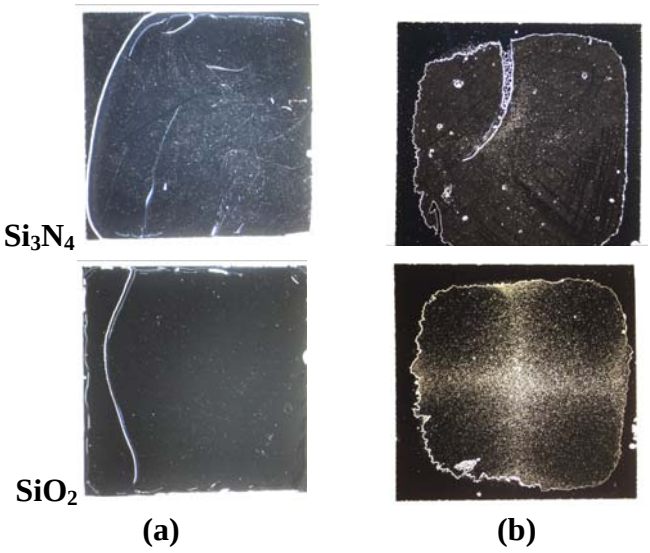

Figure 3.3: Photographs of wafer samples with Si_3N_4 or SiO_2 passivation coated with PVP (physical coating protocol) (a) before and (b) after exposure ultrasonic bath.

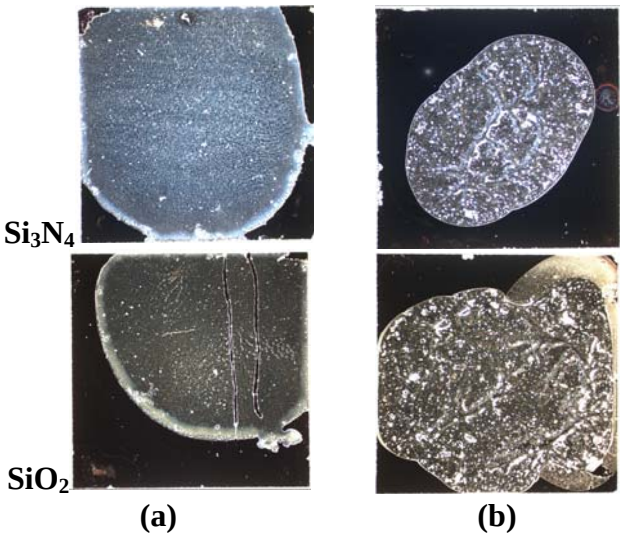

Figure 3.4: Photographs of wafer samples with Si_3N_4 or SiO_2 passivation in case of grafting-to chemical coating protocol using (a) PVP and (b) EPCO after exposure to the ultrasonic bath.

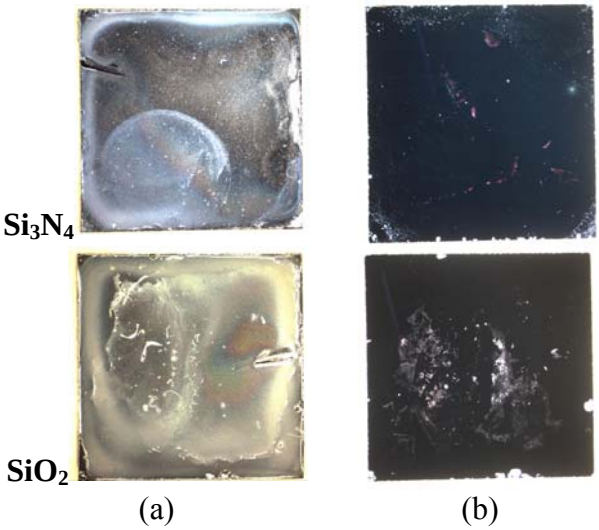

Figure 3.5: Photographs of wafer samples with Si_3N_4 or SiO_2 passivation in case of grafting-from chemical coating protocol with SBR (a) before and (b) after ultrasonic bath.

After mechanically stressing the coated samples in the ultrasonic bath, the polymer layers treated with an HMDS coupling agent exhibited the smallest amount of delamination (see Fig. 3.4). In case of the grafting-from chemical bonding method (see

Fig. 3.5), no polymer residues remained on the silicon nitride surface. However, SBR coated on the silicon dioxide surface showed some polymer residues in the center. In order to verify the thickness of the remaining coating, the film thickness was measured using a profilometer (see Figure 3.6b) and an SEM image was taken after sputter-coating the sample with a gold layer (see Figure 3.6a). The profilometer measurement indicates that some SBR coating indeed remained on the wafer sample with a silicon dioxide passivation. However, the SEM micrograph suggests that a monolayer might not have formed in the remaining areas of the wafer sample. Therefore, more detailed tests are needed in order to verify the existence of a monolayer on the surface.

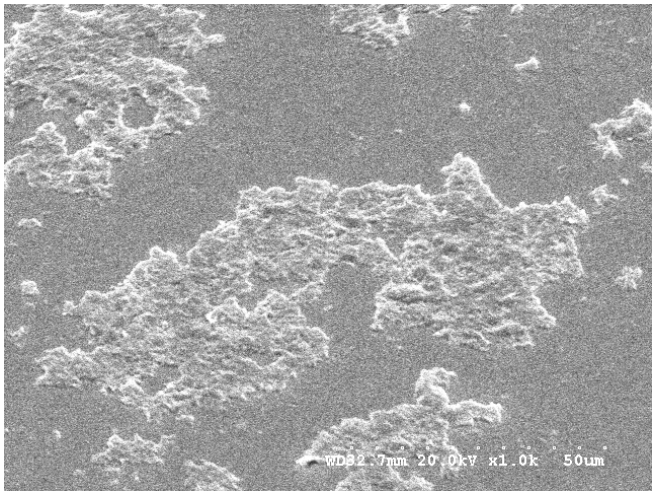

(a)

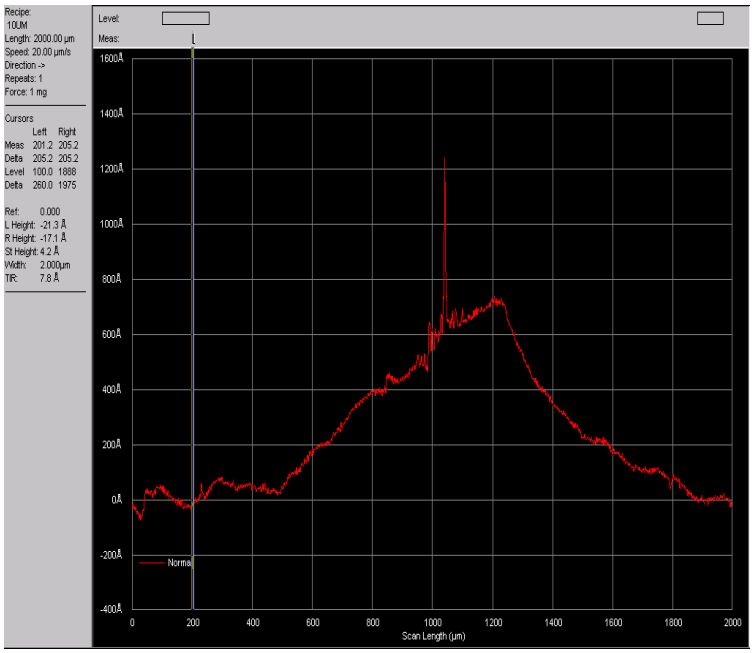

(b)

Figure 3.6: SBR coating on a SiO_2 surface after exposure to the ultrasonic bath: (a) SEM image, (b) profilometer measurement showing a remaining film thickness of approx. 70nm.

Based on the results of the adhesion tests, all resonators used in the measurement section (see Chapter 4) were treated with an HMDS coupling agent. The selection of the

volatile organic compound used as chemical analyte depends on its molecular weight, enrichment factor for the chosen polymer coating, and inertness to the tubing material. A high molecular weight and enrichment factor are desired to maximize the mass added to the resonator. The pollutant selected for this work is tetrachloroethylene (TeCE), which has a high molecular weight of 165.8 g/mol, a liquid density of 1.622 g/cm^3 and an enrichment factor in EPCO of 1200. As discussed in Chapter 4, polyetheretherketone (PEEK) was used for the tubing as well as the flow cell.

CHAPTER 4

LIQUID PHASE MEASUREMENTS

4.1 Measurement and Coating Setup

The reliability of chemical measurements in a liquid environment largely depends on the quality of the measurement setup and the stability of the sensitive layer exposed to the liquid. The measurement setup must be leak-free, allow for easy exchange of the device under test (DUT), enable injection and disposal of the analyte solutions, and comprise chemically inert materials. Packaging and test setup materials have to be carefully considered in a chemical sensing application. Even though polymers are widely used materials in microelectronic packaging, they potentially absorb analyte molecules similar to the polymer-based sensitive layers used in this work. An example is epoxies, a commonly used polymer family for the encapsulation of microelectronic circuits. Even though epoxies show relatively small partition coefficients for the analytes of interest, a potentially large surface area compared to the actual area of the sensitive film could affect the measurement results. As a compromise, poly(etheretherketone) (PEEK) was chosen as the material for the flow cell; PEEK is well known for its chemical inertness, but can still be easily machined by computer-numerically-controlled equipment.

Looking at coating techniques for the sensitive layer, one widely used method for QCMs and cantilevers is spray-coating. Here, a shadow mask generally protects area not to be coated. While uniform films can be achieved by spray coating, undesired areas, such as the side walls of the etch cavity, are coated as well, resulting in analyte

absorption in areas which do not contribute to the sensor signal. In this work, an alternative coating technique by dispensing polymer solution from a syringe was investigated. The custom designed coating system allows to only coat the surface of the resonator and potentially enables the coating of a sensor array with different sensitive layers. Moreover, the dispensing technique can be automated in the future. The developed system uses a metal microneedle and a 1.5mL plastic syringe. The coating system is attached to the bond arm of a wire bonder, which enables precise alignment under the microscope.

4.1.1 Flow Cell Design

A 3D schematic of the designed flow cell is shown in Figure 4.1. As discussed above, the flow cell must provide inlet and outlet ports for the liquid samples, must allow for easy exchange of the test chip, provide a chemically inert and leak-free enclosure of the resonator area, and a small internal sample volume. The flow cell was fabricated from PEEK, which is well-known for its chemical resistance.

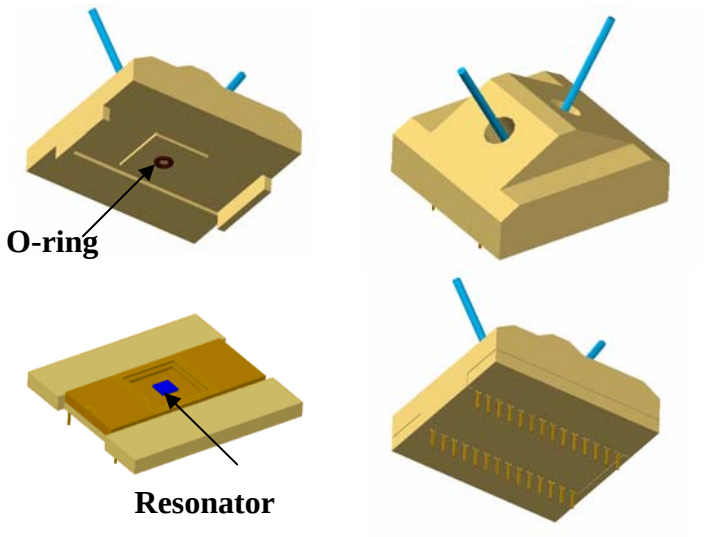

(a) (b)

Figure 4.1: 3D view of designed flow cell (a) before and (b) after assembly.

The flow cell has three components, as displayed in Figure 4.2: a top, a center alignment piece, and a base. The top part guides inflow and outflow of the liquid to the resonator. The top component has an O-ring sealing in the center, which seals it to the ceramic dual-in-line (DIL) package holding the resonator chip. The base component has 28 through-holes, which align the DIP package to the center of the base. The critical alignment between the top and base part is established by the protruded edge of the top component fitting into a cavity of the bottom component. The middle piece is only used to position the resonator in the center of the DIP during the so-called die bonding step.

Top Center Base

Figure 4. 2: Three components of designed flow cell.

Actual pictures of the three components are shown in Figure 4.3. The top and base components are attached to each other by screws and nuts on each side of the flow cell. The components have been produced using a computer-numerically-controlled milling machine. PEEK is only used for the top part, while the center and base part, which are not in contact with the sample liquid, are machined from polycarbonate. After chemical testing, the flow cell is rinsed with de-ionized water for reuse.

(a) (b)

Figure 4. 3: (a) Fabricated flow cell components and the DIL package with bonded resonator chip and (b) overall setup with flow cell mounted to circuit board holding the feedback circuitry.

4.1.2 Customized Coating System

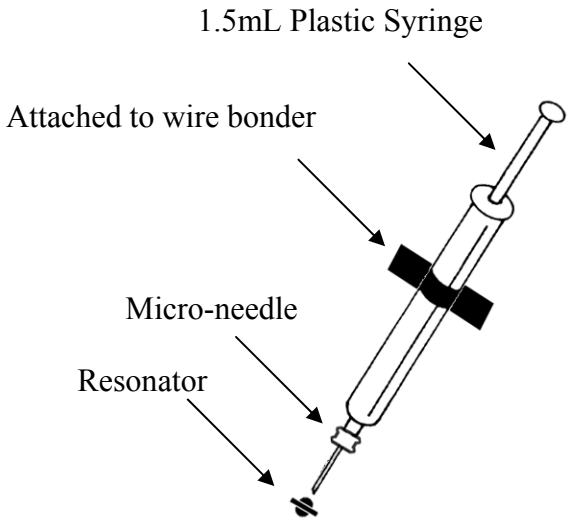

Figure 4. 4: Customized coating setup attached to wire bonder.

The first generation of the coating system used a plastic tube to connect a 1.5mL plastic syringe to a glass capillary, which was small enough to allow for local spot coating on the resonator. However, this setup often leaked and suffered from diffusion of polymer solvent in the polymer tube. An upgraded system was developed by substituting the glass capillary and tubing by a metal microneedle, which tightly fits to the plastic syringe. The inner diameter of the needle is close to 100μm which is smaller than the radius of the resonator. The plastic syringe with microneedle was attached to the bonding arm of a manual wire bonder, enabling precise alignment of microneedle and resonator under the microscope.

When depositing very small volumes of polymer dissolved in a proper solvent, the vapor pressure and viscosity of the solvent is a major concern. For successful

deposition of a very small solvent drops, the desired solvent properties are high solubility of the matching polymer, low vapor pressure, and low viscosity. Unfortunately, a tradeoff exists between the vapor pressure and the viscosity. Solvents with high vapor pressure evaporate too fast, leaving only little time for local deposition. Conversely, viscous polymers are hard to push through the microneedle making it difficult to dispense small volumes. In the present work, hexane instead of toluene was used as solvent for EPCO. Hexane has a viscosity of 0.294cP at room temperature, approximately half of the viscosity of toluene.

The manual deposition technique requires considerable training to successfully coat on the desired location on the resonator without damaging the resonator. After repeated training, the success rate of the deposition reached approximately 80%.

4.2 Measurement Results

For the measurements, the resonators are coated with a sensitive polymer layer as described above. The expected frequency change after depositing the polymer coating is calculated and compared with measurements of the resonance frequency before and after coating. Subsequently, the resonator is exposed to well-defined analyte concentrations with DI-water cycles in-between. The detection limit is calculated assuming that the minimum detectable frequency change is three times the Allan Variance, which is a measure of the short-term frequency stability of the resonator. Finally, the expected resonance frequency change after analyte injection is calculated. These calculations are compared against actual measurement data.

4.2.1 Analytical Calculation of Resonance Frequency after Polymer Coating

Using Eq. (2.2), the expected resonance frequency drop caused by the polymer coating on the resonator can be calculated. The assumptions behind this calculation are that 1) the density of polymer remains unchanged after deposition, 2) the polymer coating is uniformly distributed over the surface of the resonator, and 3) the polymer does not affect the stiffness of the resonator. Hence, the mass of the added polymer coating can be calculated by finding the volume and density of the polymer coating. The polymer thickness of a coated sample was evaluated with an atomic force microscope for one sample, and a film thickness close to 1.5μm was found.

Alternatively, the polymer thickness can be estimated using Eq. (2.2) (and assuming a uniform film thickness) from the measured frequency changes upon polymer coating. Figure 4.5 plots the estimated film thickness for EPCO and PVP films as a function as a function of the polymer concentration in the solvent. As expected, the resulting film thickness increases with increasing polymer concentration, as the deposited solvent volume is more or less constant from deposition to deposition.

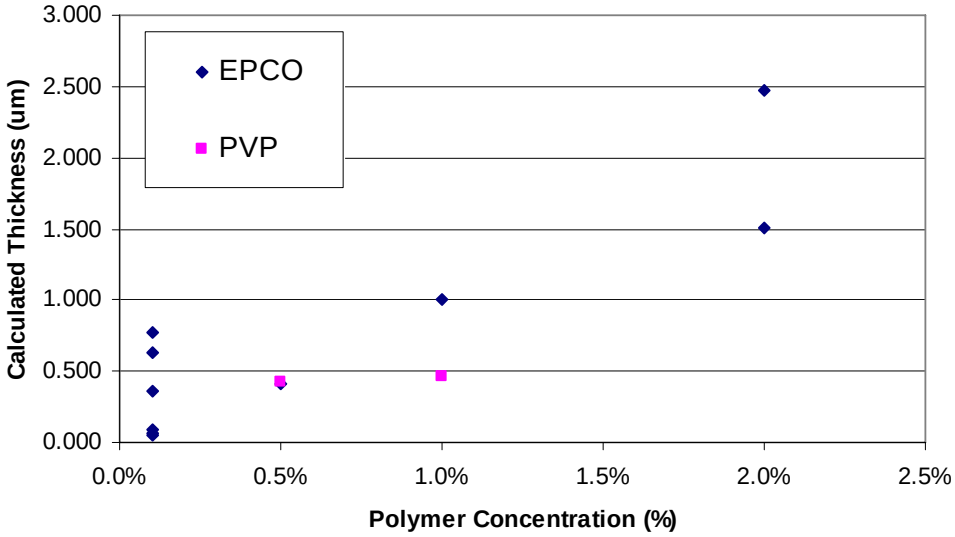

Figure 4. 5: Polymer film thickness calculated from the resonance frequency change before and after coating as a function of the polymer concentration in the solvent.

4.2.2 Estimation of Detection Limit

The minimal detectable frequency change of the disk-shape resonator operating in a closed-loop configuration can be found by using the Allan variance method [27]. The Allan variance measurement in water with 1-sec gate time was obtained from resonators with and without coating. From these data, the detection limit can be estimated. The results are summarized in Table 4.1.

Table 4. 1: Calculation of detection limit using the Allan Variance data (* the enrichment factor for PVP is estimated and needs to be verified experimentally)

Coating	Uncoated	PVP 0.5%	EPCO 0.5%
Resonator Type	1	2	3
Resonator Area (μm²)	31320	43079	42871
Resonator Mass (μg)	0.584	0.803	0.799
Resonance Frequency (kHz)	561.41	353.82	303.35
Measured Allan Variance in Liquid σ (Hz)	0.3	10.74	19.34
Minimum Frequency Resolution 3σ (Hz)	0.9	32.22	58.02
Equivalent Mass Resolution (pg)	1.872	146.248	305.635
Experimental Parameters			
TeCE Density (g/mL)	1.623	1.623	1.623
TeCE Concentration in Liquid (ppm=μL/L)	150	150	150
TeCE Concentration in Liquid (g/L)	0.243	0.243	0.243
Flow Rate (μL/min)	10	10	10
Period of Analyte Injection (min)	30	30	30
Injected Analyte per Period (μg)	73.0	73.0	73.0
Analyte Mass and Expected Frequency Change			
Enrichment Factor	N/A	200*	1200
Assumed Polymer Thickness (μm)	N/A	0.5	0.5
Volume of Polymer (μm³)	N/A	21539	21436
Analyte Mass in Polymer (ng)	N/A	1.05	6.25
Expected Frequency Change (Hz)	N/A	231	1188

The data summarized in Table 4.1 leads to the following observations and conclusions:

1. The measured Allan variance in liquid is strongly affected by the polymer coating: with polymer coating, the short-term frequency stability and thus the mass resolution degrades by 1-2 orders of magnitude. The reason for this is unclear at the moment and must be subject to further investigations.
2. Even with the measured frequency stabilities of polymer-coated resonators in liquid, a TeCE concentration of 100 ppm should be easily detectable.

3. If the adhesion problems can be solved and a frequency stability similar to the uncoated resonator can be achieved in liquid, sub-ppm concentrations of TeCE should be detectable with a 0.5µm EPCO film as sensitive layer.

The total injected mass of the analyte (TeCE) for a given experimental cycle is calculated using

$$m_{TeCEtotal} = t_{inj} \times v_{flow} \times c_{liquid} \times \rho_{analyte} \qquad \text{Eq. (4.1)}$$

where t_{inj}, v_{flow}, c_{liquid}, and $\rho_{analyte}$ denote injection time, flow rate, analyte concentration in the liquid, and analyte density, respectively. The total injected analyte mass in a measurement cycle must be much larger than the mass uptake in the polymer to ensure that an equilibrium is reached and that the analyte is not depleted considerably from the liquid phase.

4.2.3 Measurements with PVP Polymer Coating

Before running the actual liquid-phase measurement, the device is characterized in air using a network/spectrum analyzer (Agilent 4395A) before and after polymer coating. Appropriate excitation signals are applied to the heating resistors and the output of the piezoresistive Wheatstone bridge is measured [14]. The network/spectrum analyzer records the amplitude and phase transfer characteristic around the rotational in-plane resonance mode of the resonator. The amplitude/phase transfer characteristics before and

after coating the resonator with PVP (using a 0.5% PVP solution) are displayed in Figure 4.6.

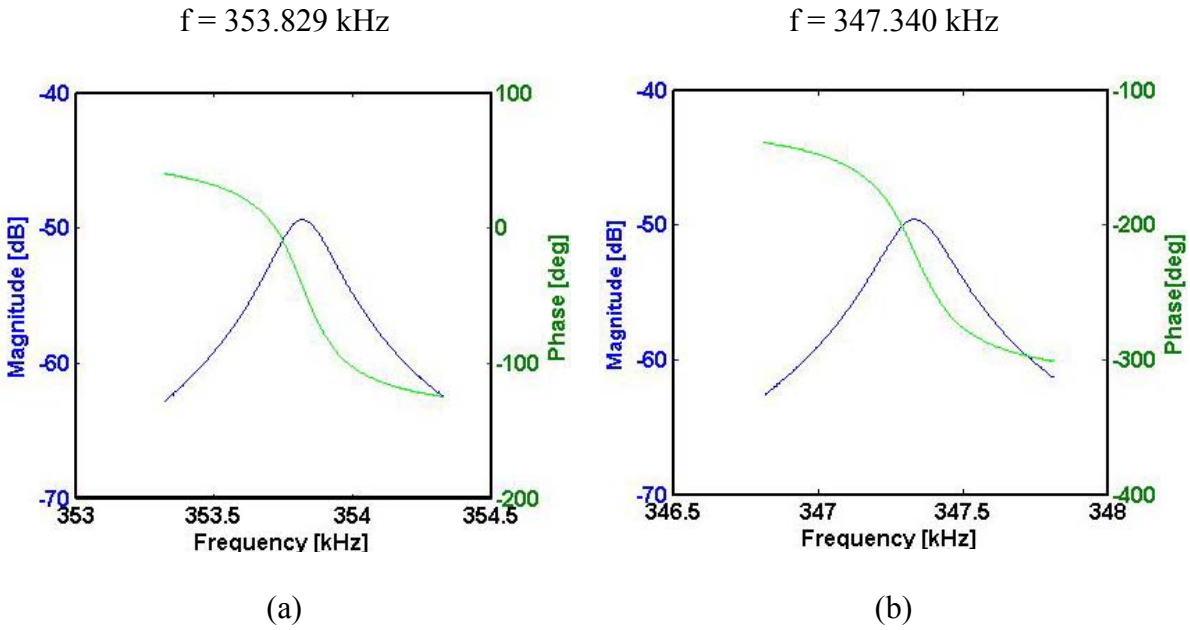

Figure 4. 6: Magnitude and phase transfer characteristic in air around in-plane resonance mode (a) before and (b) after coating with PVP film.

Figure 4.7 shows optical images of the resonator taken before coating, after coating with PVP, and after measurement in liquid. The images indicate non-uniform polymer film properties, but also a good stability upon liquid exposure. Some delamination of the PVP coating was observed even though no adhesion loss was found at the interface layer of the PVP coating. In fact, after the measurements in water, some of the PVP accumulated near the gap between semi-disk and anchor beam (see arrow in Figure 4.7c).

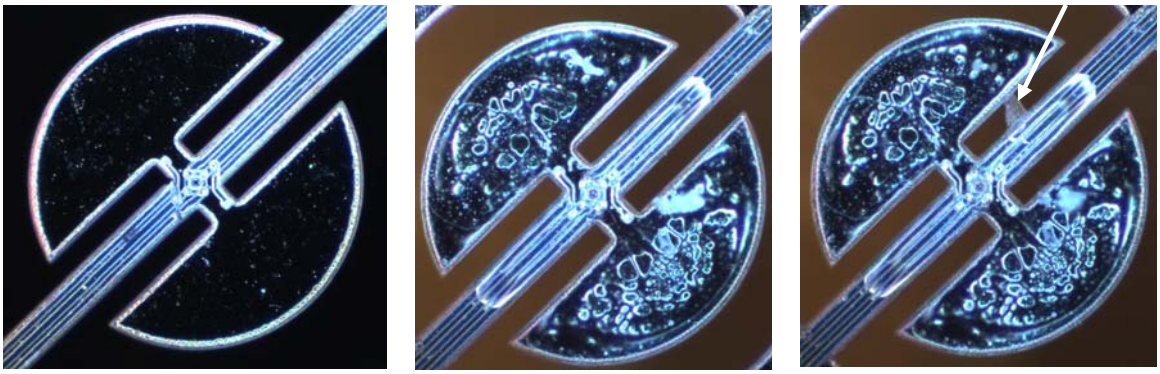

(a) (b) (c)

Figure 4. 7: Photographs of disk-type resonator taken (a) before coating, (b) after coating with 0.5% PVP, and (c) after liquid measurement.

Figure 4.8 shows the response of the resonator, i.e. the change of the resonance frequency, to periodic injections of 30ppm TeCE in DI water. The overall flow rate is held constant at 8µl/min and analyte solution is periodically injected for 30min, followed by 60min injection of DI water. No clear responses to the analyte injection can be observed. While the short-term frequency stability is fairly good during the measurement, it suffers from occasional large steps in the resonance frequency, which are potentially associated with air bubbles in the flow chamber. Alternatively, the polymer residues between semi-disk and anchor beam could be the reason for the frequency steps. A decrease in frequency upon analyte injection, as seen once during the measurement (see arrow in Figure 4.9), is expected. However, this result could not be observed repeatedly.

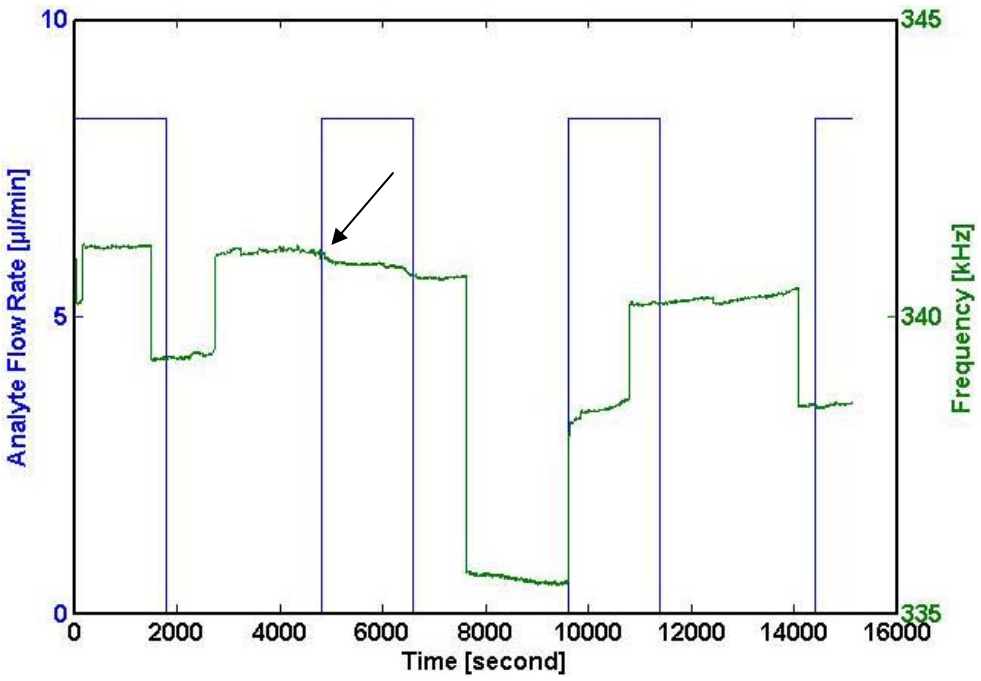

Figure 4. 8: Resonance frequency of disk-shape resonator coated with PVP film in water subject to periodic injection of 30ppm TeCE.

Another measurement was conducted with a PVP-coated resonator. This time the polymer film was dispensed from a 1% PVP solution to yield a larger polymer thickness and the concentration of TeCE was increased from 30ppm to 150ppm to induce a larger analyte absorption in the polymer film , thus, a larger sensor sensitivity. Figure 4.9 shows the amplitude/phase transfer characteristic of the device in air before and after polymer coating. As expected, a larger polymer mass could be deposited, indicated by the larger relative frequency shift observed in Figure 4.9 compared to Figure 4.6. Photographs of the resonator before coating and after coating and liquid measurements are given in Figure 4.10. After liquid-phase measurements, polymer residues are clearly visible in the gap between semi-disks and anchor beam. It is believed that these polymer residues are at least partly responsible for the observed instabilities during the measurement in liquid

(see Figure 4.11). During the measurement it was observed that frequency stability degraded as the liquid measurement time progressed.

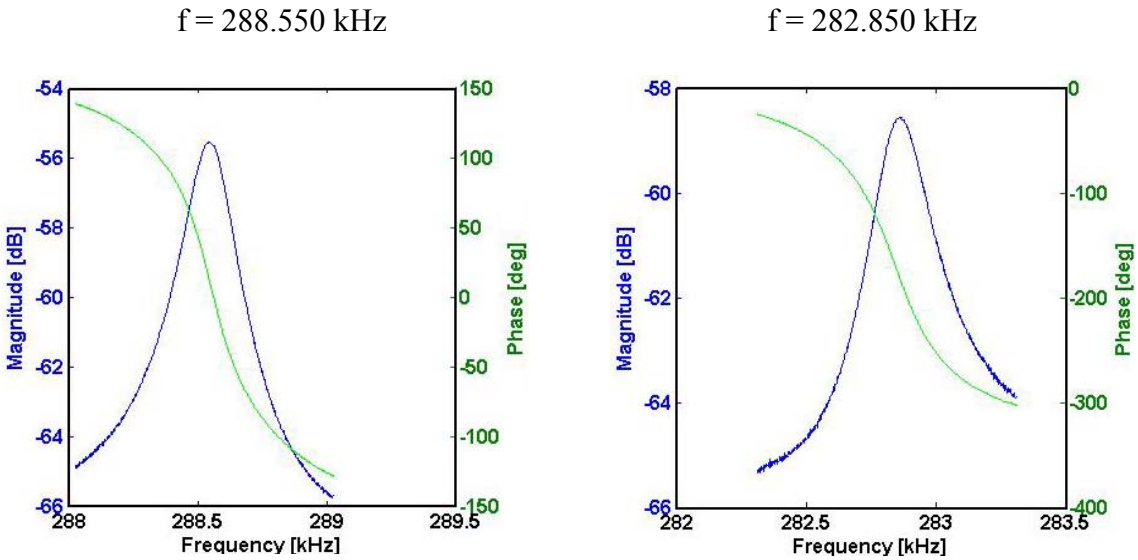

(a) (b)

Figure 4. 9: Magnitude and phase transfer characteristic in air around in-plane resonance mode (a) before and (b) after coating with PVP film deposited from 1% PVP solution.

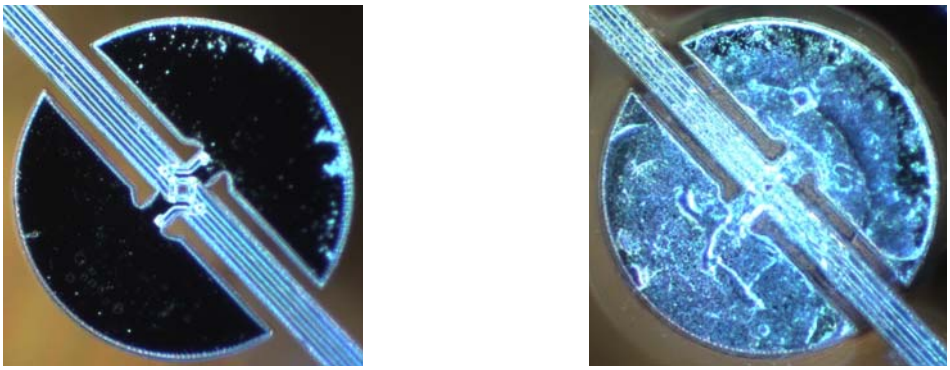

(a) (b)

Figure 4. 10: Photographs of disk-type resonator taken (a) before coating, (b) after coating with 1% PVP and liquid measurement.

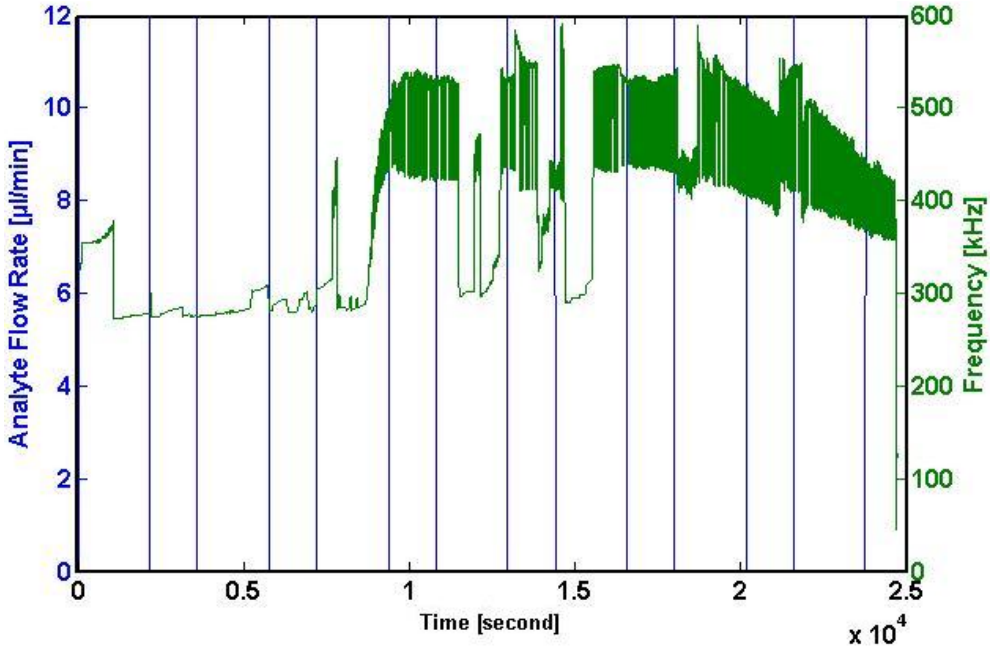

Figure 4. 11: Resonance frequency of disk-shape resonator coated with PVP film (deposited from 1% PVP solution) in water subject to periodic injection of 150ppm TeCE.

4.2.4 Measurements with EPCO Polymer Coating

Alterative to the PVP coating, disk-type resonators with an EPCO coating were tested. EPCO exhibits higher enrichment factor for TeCE in water, with typical values between 1000-1500 at room temperature. Since the enrichment factor for TeCE in EPCO is higher than in PVP, larger frequency shifts in response to the analyte injection were expected (see also Table 4.1). The device used for this measurement was coated from a 0.5% EPCO solution using hexane as solvent. Figure 4.12 shows amplitude/phase transfer characteristics before and after polymer coating.

f = 303.355 kHz

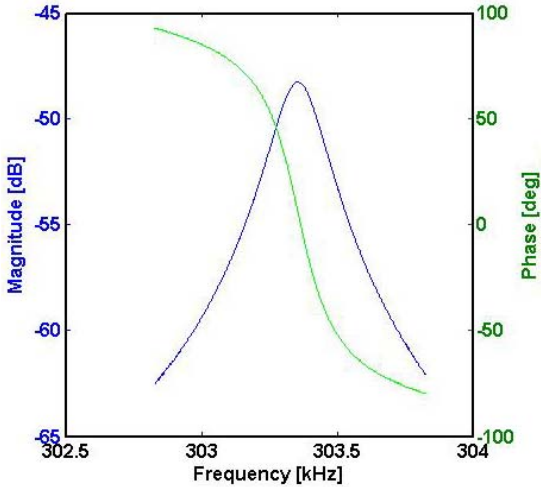

(a)

f = 413.920 kHz

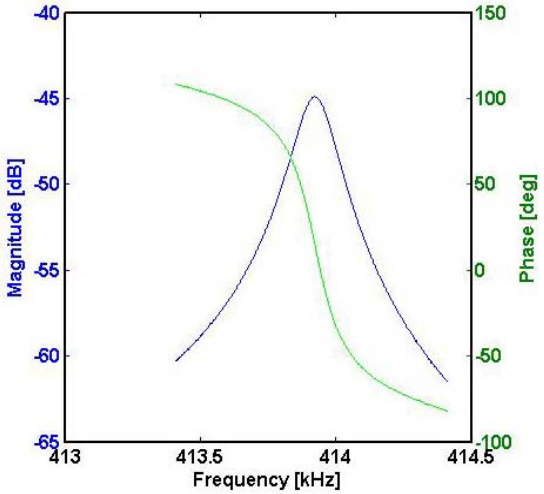

(b)

Figure 4. 12: Magnitude and phase transfer characteristic in air around in-plane resonance mode (a) before and (b) after coating with EPCO film deposited from 0.5% EPCO solution in hexane.

After operating the resonator in liquid, polymer residues in the air gap are clearly visible similar to the PVP-coated sensors, as shown in Figure 4.13. Since the glass transition temperature of EPCO is lower than the operating temperature, EPCO is expected to act like a rubbery polymer with fast response time. However, as shown in Figure 4.13, rubbery polymers, such as EPCO, seems to be more affected by the in-plane movement of the resonator, which is associated with surface shear forces.

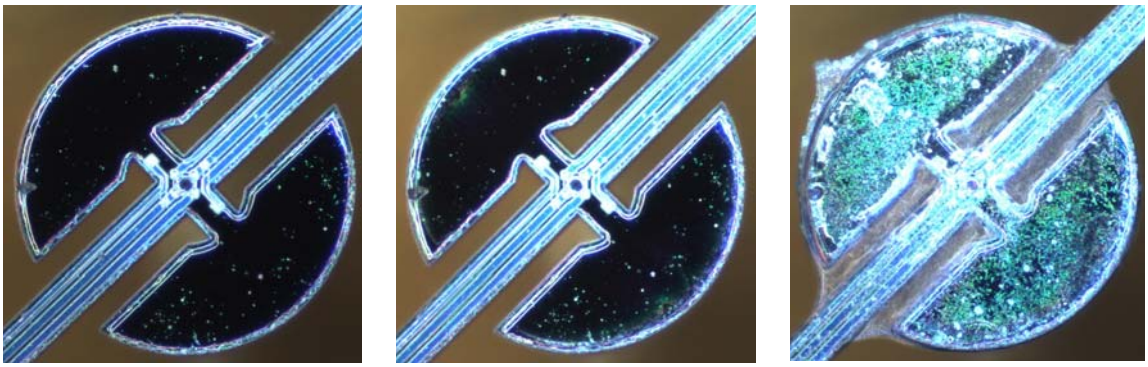

(a) (b) (c)

Figure 4. 13: Photographs of disk-type resonator taken (a) before coating, (b) after coating with 0.5% EPCO solution and (c) after liquid measurement.

Figure 4.14 shows the resonance frequency of the EPCO-coated resonator over time, subject to periodic exposure to 150ppm TeCE in DI water. The noise level observed in this measurement was distinctly higher than for the measurements with the PVP-coated sensors. It should be pointed out, however, that a frequency shift upon analyte exposure of several kHz was expected for this measurement. Again, no reproducible change in resonance frequency upon analyte exposure could be detected. It is suspected that due to the polymer softening after analyte injection the mass loading on the polymer was not completely coupled onto the resonator, therefore limiting the effect of the added mass.

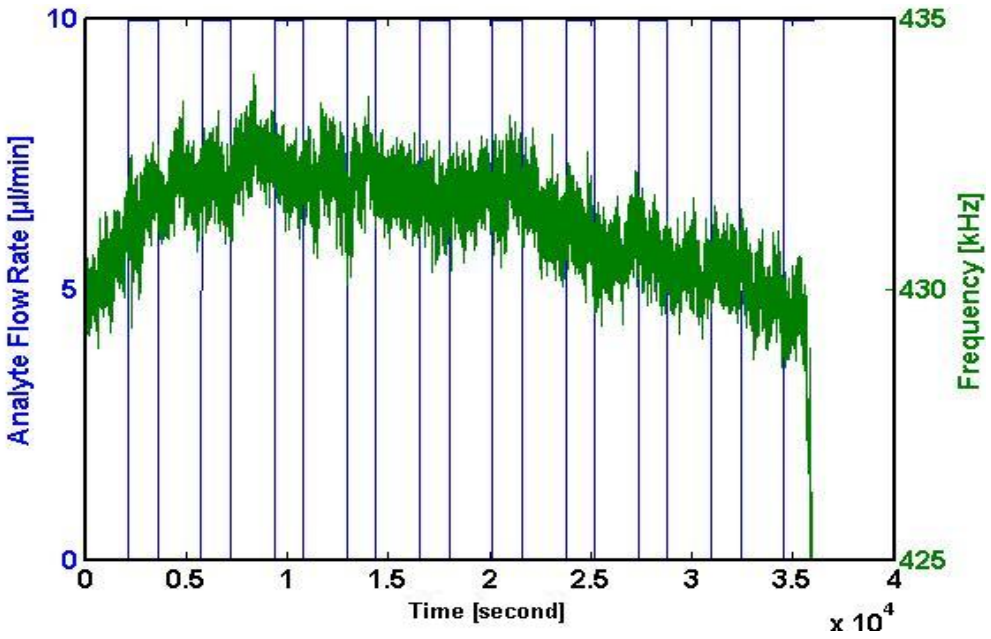

Figure 4. 14: Resonance frequency of disk-shape resonator coated with EPCO film (deposited from 0.5% EPCO solution) in water subject to periodic injection of 150ppm TeCE.

In order to minimize the potential effect of the shear mode resonance on the characteristics of the polymer film, a thinner layer was deposited from a 0.1% EPCO solution in hexane. However, the noise level was too high to test with TeCE analyte injection. The amplitude/phase transfer characteristic of the device in air is shown in Figure 4.15 before and after polymer coating.

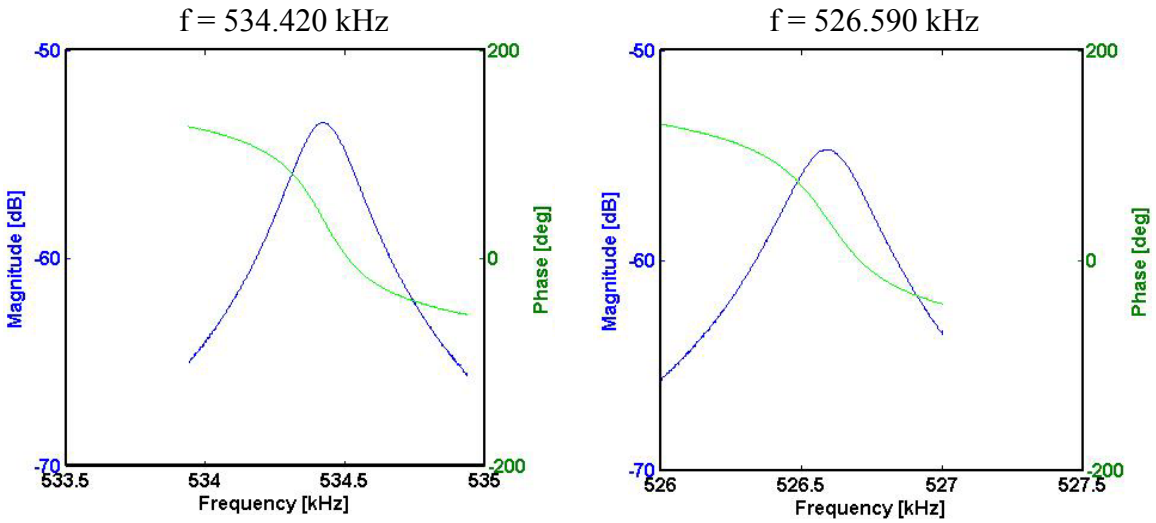

Figure 4. 15: Magnitude and phase transfer characteristic in air around in-plane resonance mode (a) before and (b) after coating with EPCO film deposited from 0.1% EPCO solution in hexane.

Images of the resonator before coating, after polymer coating and after liquid operation are summarized in Figure 4.16. While the air gap is not clogged with polymer residues, a large residue adhering to one of the semi-disks might cause the observed frequency instabilities.

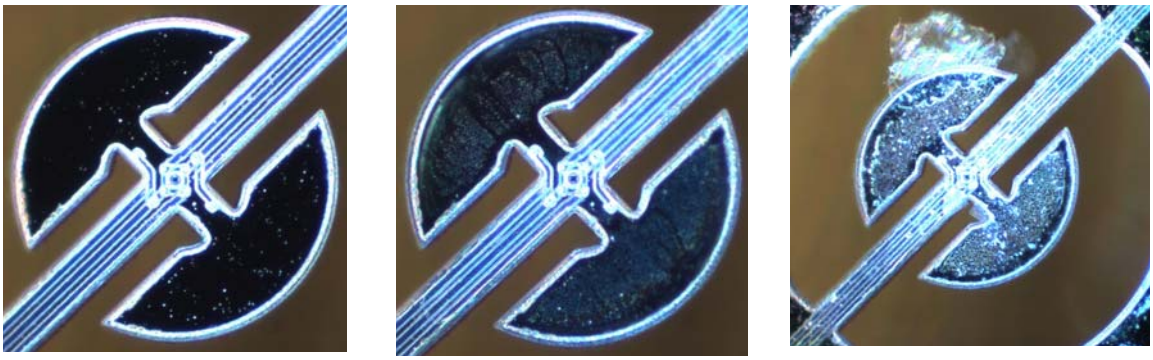

(a) (b) (c)

Figure 4. 16: Photographs of disk-type resonator taken (a) before coating, (b) after coating with 0.1% EPCO solution and (c) after liquid measurement.

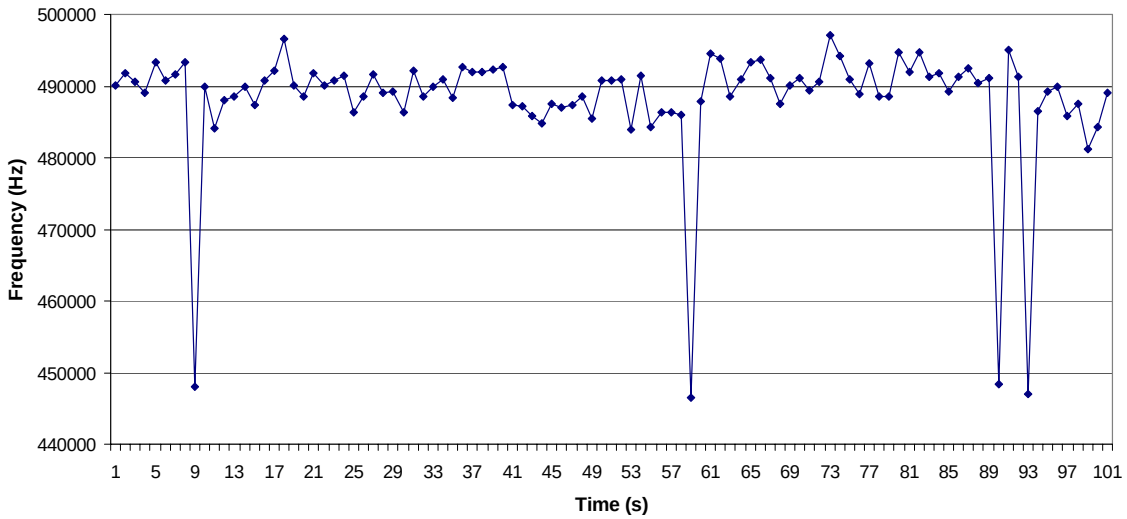

Figure 4. 17: Measured resonance frequency during 100s period for EPCO-coated resonator (deposited from 0.1% EPCO solution).

4.2.5 Testing of Uncoated Resonator in Liquid Flow Cell

To investigate the origin of the observed frequency instabilities, an uncoated resonator with a resonance frequency of 561.42kHz was tested in water at a constant flow rate of 10µl/min. Over several hours, the measured resonance frequency increases gradually, as shown in Figure 4.18.

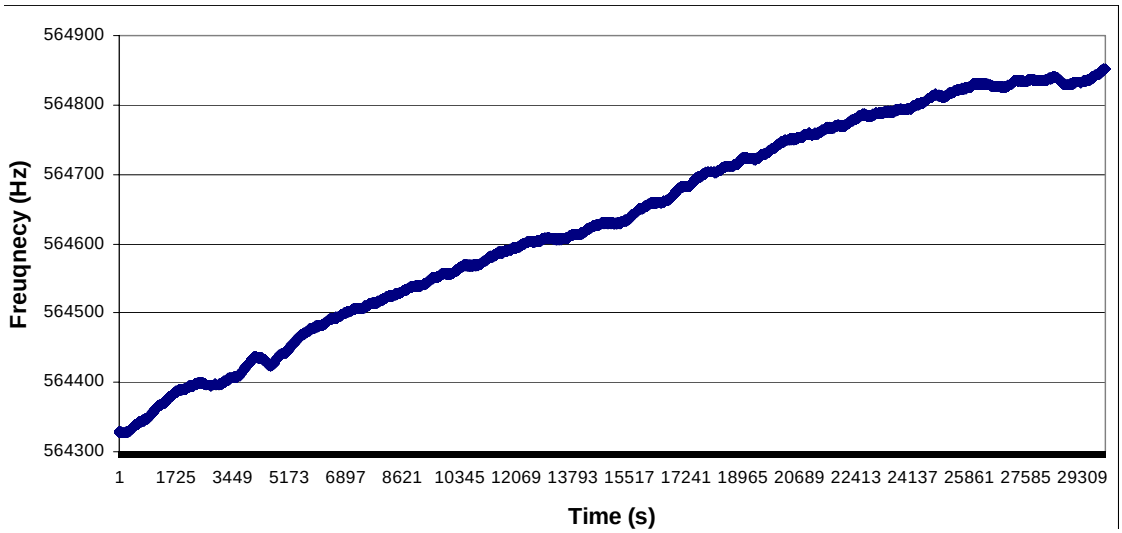

Figure 4. 18: Frequency measurement of uncoated resonator during equilibration in liquid flow cell with 10µl/min flow rate.

The short-term frequency stabilities of the coated and uncoated resonators are compared by observing the frequency fluctuations in a short time period of 100s. By comparing Figure 4.17 and Figure 4.19, it is clearly visible that the short-term frequency stability of the uncoated device is approximately 10,000 times better than that of the coated device. Thus, the short-term frequency stability seems to be clearly affected by the polymer coating.

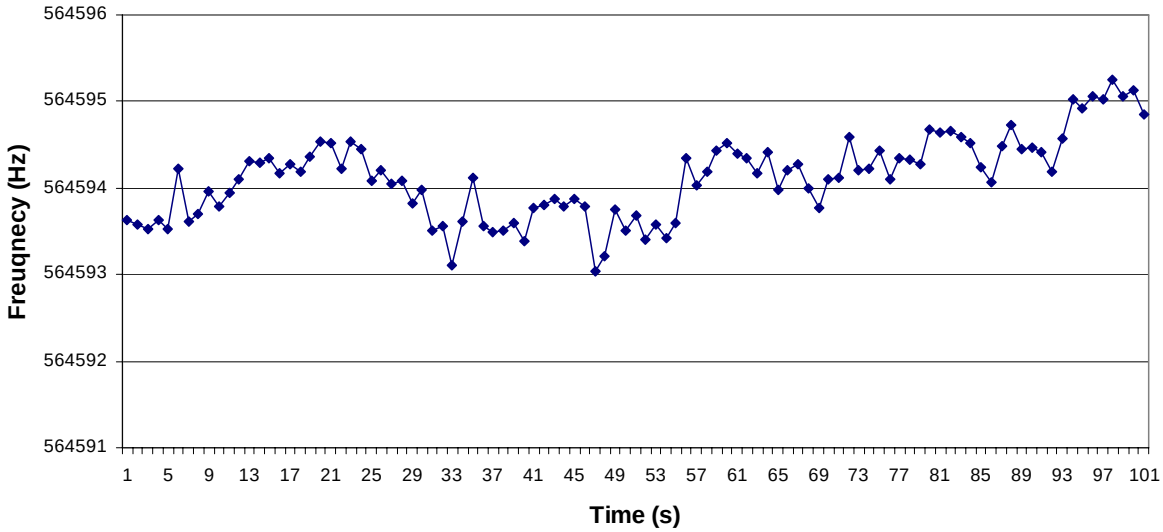

Figure 4. 19: Measured resonance frequency during 100s period for uncoated resonator.

CHAPTER 5
CONCLUSIONS AND RECOMENDATIONS

5.1 Conclusions

Many issues related to the liquid-phase chemical measurement have been identified and solved in the process of reaching the final stage of this work, namely measurements with actual analyte injection. The detachable flow cell allows continuous monitoring of the condition of the resonator even while running the actual measurement and the chemically inert properties of the flow cell material minimize its effect on the measurement. The reusability of the flow cell ensures a consistent volume of the sampling chamber for all measurement and, thus, improves the reliability of the measurement data.

The possible delamination of the polymer coating was addressed in the early stages of this research and several solutions have been proposed to solve this problem. The interfacial moisture between the polymer and substrate was identified as the source of adhesion failure and physical and chemical binding methods have been investigated to improve film adhesion. As an example, the resonator surface was pretreated with an HMDS coupling agent, which increases the hydrophobicity of the surface, reduces the water diffusion along the interface and generally improves adhesion.

To improve the repeatability of the local deposition method, a simple customized coating system was developed by attaching a plastic syringe with microneedle to the probe arm of a wire bonder allowing for precise alignment. Through a series of

optimization processes including lowering the polymer concentration, using less viscous polymer solvents with low vapor pressure and, last but not least, personal training, the reliability and repeatability of the polymer coating process was improved. Local deposition of the sensitive layer only on the disk area of the resonator is achieved, thus eliminating undesirable analyte enrichment in non-active areas.

Compared to gas-phase measurements, liquid-phase measurements using resonant microsensors introduce additional measurement challenges. In the liquid, the damping by the environment is strongly increased, lowering the quality factor of the resonance, thus reducing the frequency stability and ultimately the sensor sensitivity. Moreover, due to the high dielectric constant of water compared to air, the degree of (capacitive) cross-talk from the excitation signal to the readout signal of the microresonator significantly increases, making it hard to fine tune the phase in the amplifying feedback loop. In addition, heating of electronic components on the printed circuit board adds additional phase shift in the closed-feedback loop, forcing the resonator to operate at less optimum conditions.

Looking at the experimental data presented in this work, two main challenges preventing repeatable chemical measurements can be identified:

1. The frequency stability of the resonators is degraded by at least two orders of magnitude once the sensors are coated with the polymer sensitive film. The source of the observed instabilities in the frequency measurement is likely a combination of multiple factors, such as the instability of the polymer film, trapping of air bubbles during measurement, pressure steps created by the used syringe pumps, and viscosity effects due fluid motion in the sample chamber.

2. During operation in a liquid environment, polymer material apparently migrates to areas of minimal displacement, i.e. in particular towards the air gaps between the semi-disks and the central anchor beam. The accumulation of polymer in the air gaps is more pronounced in case of rubbery polymers and for larger film thicknesses. Polymeric material bridging the air gap increases the stiffness of the resonator and might be responsible for the slow increase in resonance frequency with time observed for some of the resonators.

The polymer coated in-plane resonators might suffer from a film resonance effect originally observed in shear-mode acoustic wave devices [9]. The film resonance effect occurs as the temperature is raised and the effective modulus of the polymer layer decreases. During oscillation, the upper surface of the polymer film lags behind the motion of the lower parts of the polymer film close to the device interface. This phase lag induces strain across the thickness of the film and dissipates energy. This energy loss decreases the quality factor of the coated resonator, which would result in a degraded (short-term) frequency stability. Additionally, the phase lag along the thickness of the film might cause the upper polymer layers to migrate towards area of reduced shear forces.

While attempting to reduce the polymer migration in water and improve the short-term frequency stability, tradeoffs will likely have to be made between analyte absorption, sensor sensitivity and resolution on one side, and adhesion strength in liquid, inertness to the shear mode resonance and relaxation time one the other hand. While further investigations are essential, the following trends are visible from the gathered experimental data: Glassy polymers, such as PVP, seem to exhibit a higher adhesion

strength in liquids, a higher inertness to the shear mode resonance, and a higher quality factor since less energy is dissipated through coupling with the polymer, but generally have slower response times and enrichment factors. On the other hand, rubbery polymers, such as EPCO and SBR, tend to show fast response times and high analyte absorption, but have weaker adhesion strength and shear strengths, larger relaxation time and, therefore, exhibit an increased energy loss through coupling with the polymer film. Therefore, the quality factor of identical resonators coated with EPCO will be lower than that of resonators coated with PVP [11].

Unfortunately, lessons learned for other chemical sensing techniques used in the liquid phase are not necessarily applicable to the present mass-sensitive sensor principle. As an example, rubbery polymers, such as EPCO and SBR, generally outperform glassy polymers, such as PVP, in static measurement principles, such as infrared spectroscopy. However, in these static sensing techniques, the polymer sensing film is not sheared and adhesion strength in liquid, inertness to shear mode resonance or relaxation time are not a concern. For dynamic measurements operation, these factors become important and a good enrichment factor should potentially be traded off for stability in the measurement. To complicate things even more, the mechanical material properties of the polymer coating might change upon analyte absorption. It is known that analyte absorption in polymers is usually accompanied by material softening, a decrease in shear modulus at high frequencies, and a decrease of the glass transition temperature [11].

5.2 Recommendations for Future Work

The main issues to be addressed in the future work are the frequency stability of the polymer-coated resonators in liquid and the polymer migration during liquid operation. It is believed that the instability contributed by the polymer film can be drastically reduced if the polymer coating method creates a tightly bound monolayer. The grafting-from chemical bonding technique discussed earlier can be a promising solution for both monolayer deposition and selective coating. Using UV activated photo-linkers it is possible to create surfaces that have very low surface free energies with a good degree of control in thickness, adhesion, and composition of the coating [24]. However, systematic verification other than the SEM images used in this work should be employed to characterize the properties of the deposited monolayers. Another common technique is the use of gold-coated sensor surfaces in conjunction with thiol chemistries to deposit self-assembled monolayers.

When designing future resonant microstructures for chemical sensor applications, the design should consider ease of polymer deposition, packaging, and testing. A design that is less sensitive to e.g. air bubbles potentially improves the measurement stability. On the other hand, the liquid flow around the resonator must be considered already at the design stage. The current disk-type resonator is surrounded by a 100 μm gap, which is too small to allow a good fluid flow around the microstructure. Finally, additional challenges might appear if we step from individual sensors to sensor arrays. During the measurements, we observed the polymer material not only migrated to the air gaps between semi-disks and anchor beam, but also to uncoated reference sensors in the vicinity.

REFERENCES

1. Hierlemann, A., et al., *Microfabrication techniques for chemical/biosensors.* Proceedings of the IEEE, 2003. **91**(6): p. 839-863.

2. Weetall, H.H., *Editorial.* Biosensors and Bioelectronics, 1999. **14**(2): p. 237-242.

3. Hagleitner, C., et al., *Smart single-chip gas sensor microsystem.* Nature, 2001. **414**(6861): p. 293-296.

4. Baltes, H., et al. *CMOS MEMS - present and future*. 2002.

5. Wilson, D.M., et al., *Chemical sensors for portable, handheld field instruments.* Sensors Journal, IEEE, 2001. **1**(4): p. 256-274.

6. Janata, J., et al., *Chemical Sensors.* Anal. Chem., 1998. **70**(12): p. 179-208.

7. Wu, G., et al., *Bioassay of prostate-specific antigen (PSA) using microcantilevers.* Nat Biotech, 2001. **19**(9): p. 856-860.

8. Vidic, A., D. Then, and C. Ziegler, *A new cantilever system for gas and liquid sensing.* Ultramicroscopy, 2003. **97**(1-4): p. 407-416.

9. Jay W. Grate, G.C.F., *Acoustic Wave Sensors.* Sensors Update, 1996. **2**(1): p. 37-83.

10. Ali, Z., *Acoustic Wave Mass Sensors.* Journal of Thermal Analysis and Calorimetry, 1999. **55**(2): p. 397-412.

11. Lucklum, R., et al., *On-line detection of organic pollutants in water by thickness shear mode resonators.* Sensors and Actuators B: Chemical, 1996. **35**(1-3): p. 103-111.

12. Rosler, S., et al., *Sensor system for the detection of organic pollutants in water by thickness shear mode resonators.* Sensors and Actuators B: Chemical, 1998. **48**(1-3): p. 415-424.

13. Jae Hyeong, S., *Silicon-Based Resonant Microsensor Platform*, in *Electrical and Computer Engineering*. 2006, Georgia Institute of Technology: Atlanta. p. 87.

14. Jae Hyeong, S. and O. Brand. *Novel high Q-factor resonant microsensor platform for chemical and biological applications*. 2005.

15. Kinloch, A.J., *Adhesion and adhesives : science and technology*. 1987, New York: Chapman and Hall.

16. E. P. O'Brien, C.C.W.B.D.V., *Correlating Interfacial Moisture Content and Adhesive Fracture Energy of Polymer Coatings on Different Surfaces.* Advanced Engineering Materials, 2006. **8**(1-2): p. 114-118.

17. Zanni-Deffarges, M.P. and M.E.R. Shanahan, *Diffusion of water into an epoxy adhesive: comparison between bulk behaviour and adhesive joints.* International Journal of Adhesion and Adhesives, 1995. **15**(3): p. 137-142.

18. Steven H. McKnight, J.W.G., Jr., *In situ examination of water diffusion to the polypropylene-silane interface using FTIR-ATR.* Journal of Applied Polymer Science, 1997. **64**(10): p. 1971-1985.

19. Nguyen, T.B., W. E.; Alsheh, D.; McDonough, W.; Seiler, J. F., Jr., *Interfacial Water and Adhesion Loss of Polymer Coatings on a Siliceous Substrate.* Materials Research Society Symposium Proceedings, 1995. **385**(1995): p. 7.

20. Plueddemann, E.P., *Silane coupling agents / Edwin P. Plueddemann.* 2nd ed. ed, New York :: Plenum Press,. xi, 253 p. :.

21. Cassu, S.N. and M.I. Felisberti, *Poly(vinyl alcohol) and poly(vinylpyrrolidone) blends: 2. Study of relaxations by dynamic mechanical analysis.* Polymer, 1999. **40**(17): p. 4845-4851.

22. M. Pyda, M.L.D.L.J.P.P.K.A.B.J.G.B.W., *Reversible and irreversible heat capacity of poly[carbonyl(ethylene-<I>co</I>-propylene)] by temperature-modulated calorimetry.* Journal of Polymer Science Part B: Polymer Physics, 2001. **39**(14): p. 1565-1577.

23. Yukitoshi Takeshita, T.I.S.N., *Physical properties and structure of a poly(styrene-<I>co</I>-butadiene) rubber/poly(acrylonitrile-<I>co</I>-butadiene) rubber latex mixture film.* Journal of Polymer Science Part A: Polymer Chemistry, 1998. **36**(14): p. 2493-2501.

24. JeyaprakashS.Samuel, J.D. and J. Ruhe, *A Facile Photochemical Surface Modification Technique for the Generation of Microstructured Fluorinated Surfaces.* Langmuir, 2004. **20**(23): p. 10080-10085.

25. Hair, M.L. and W. Hertl, *Reaction of hexamethyldisilazane with silica.* J. Phys. Chem., 1971. **75**(14): p. 2181-2185.

26. Steven E. Sloop, M.M.L.T.S.S.A.L.T.D.G.P.J.D.S.-S., *Cross-linking poly(ethylene oxide) and poly[oxymethylene-oligo(oxyethylene)] with ultraviolet radiation.* Journal of Applied Polymer Science, 1994. **53**(12): p. 1563-1572.

27. Allan, D.W. and J.A. Barnes. *A modified `Allan variance' with increased oscillator characterization ability*. 1981. Philadelphia, PA, USA: Electron. Ind. Assoc.